REPORT DOCUMENTATION PAGE

Form Approved
OMB No. 0704-0188

1. REPORT DATE (DD-MM-YYYY)	2. REPORT TYPE	3. DATES COVERED (From - To)
09-06-2003	Technical Paper	

4. TITLE AND SUBTITLE

Microsecond Timescale Surface Temperature Measurements in Micro-Pulsed Plasma Thrusters

5a. CONTRACT NUMBER
F04611-99-C-0025

5b. GRANT NUMBER

5c. PROGRAM ELEMENT NUMBER

6. AUTHOR(S)

Erik Antonsen (ERC); Rodney L. Burton (Univ. of IL at Urbana); Gregory G. Spanjers (AFRL/VS); Ronald A. Spores (AFRL/PRSS)

5d. PROJECT NUMBER
2308

5e. TASK NUMBER
M4S7

5f. WORK UNIT NUMBER

7. PERFORMING ORGANIZATION NAME(S) AND ADDRESS(ES)

ERC
10 East Saturn Blvd.
Edwards AFB CA 93525-7680

8. PERFORMING ORGANIZATION REPORT NUMBER

9. SPONSORING / MONITORING AGENCY NAME(S) AND ADDRESS(ES)

Air Force Research Laboratory (AFMC)
AFRL/PRS
5 Pollux Drive
Edwards AFB CA 93524-7048

10. SPONSOR/MONITOR'S ACRONYM(S)

11. SPONSOR/MONITOR'S NUMBER(S)
AFRL-PR-ED-TP-2003-190

12. DISTRIBUTION / AVAILABILITY STATEMENT

Approved for public release; distribution unlimited.

13. SUPPLEMENTARY NOTES

For presentation at the AIAA Joint Propulsion Conference in Huntsville, AL, taking place 20-23 July 2003.

14. ABSTRACT

15. SUBJECT TERMS

16. SECURITY CLASSIFICATION OF:			17. LIMITATION OF ABSTRACT	18. NUMBER OF PAGES	19a. NAME OF RESPONSIBLE PERSON
					Leilani Richardson
a. REPORT	b. ABSTRACT	c. THIS PAGE	A	8	19b. TELEPHONE NUMBER (include area code)
Unclassified	Unclassified	Unclassified			(661) 275-5015

Microsecond Timescale Surface Temperature Measurements in micro-Pulsed Plasma Thrusters

Erik L. Antonsen* **and Rodney L. Burton****
University of Illinois at Urbana-Champaign IL 61801
eantonse@uiuc.edu

Gregory G. Spanjers† **and Ronald A. Spores‡**
AFRL Propulsion Directorate, Edwards AFB CA 93524

AIAA 2003-5167

A time-resolved surface temperature diagnostic for ablation-controlled arcs is in development at the Air Force Research Laboratory at Edwards AFB. The diagnostic draws on heritage from the experimental dynamic crack propagation community which has used photovoltaic infrared detectors to measure temperature rise in materials in the process of fracture. The microsecond time scales involved in the fracture process suggest that such detectors may be applicable to the ablation-controlled discharges in pulsed plasma thrusters as a direct measurement of surface temperature during and after the arc. HgCdTe detectors are evaluated for use on the surface of a micro-pulsed plasma thruster invented at the AFRL. Evaluation of the diagnostic focuses on development of valid calibration methodology and application of the detector in the presence of a plasma. Current calibration techniques are reviewed with physical limitations discussed. Detector response to an operating thruster is examined and future studies involving surface roughness changes are investigated.

Introduction

With the increasing presence of micro-propulsion options for spacecraft attitude control and propulsion, there is a corresponding need for the development of experimental techniques to better understand the operating physics of these devices. The Air Force Research Laboratory is currently developing a class of Micro-Pulsed Plasma Thrusters (MicroPPTs) using Teflon™ propellant to provide precise impulse bits in the 10 μN-s range. In the near term, these thrusters can provide propulsive attitude control on 150-kg class spacecraft at one-tenth the dry mass of conventional torque rods and reaction wheels.[1]

However, the micro-PPT still suffers the same deficiencies that standard PPTs have been dealing with since their inception. Low mass utilization coupled with spacecraft contamination concerns provide a continuing emphasis for research to improve these systems. Ultimately, post-pulse late-time ablation (LTA) in these thrusters defines operation and performance capability by sustaining significant propellant mass loss per pulse that fails to contribute to thrust. This LTA factor has been estimated between 40-90% of the total mass loss from various sources.[2,3]

Significant research effort has been expended attempting to characterize LTA in terms of plume effects both from neutral vapor interferometric measurements[4] and analysis of macro-particle ejection.[2] Past experiments have demonstrated a correlation between propellant temperature and thruster operating efficiency. Spanjers et al. inserted thermocouples into the Teflon propellant of parallel-plate PPTs to varying depths from the fuel face to measure steady-state operation temperatures at long times.[5] Of note from

---

*Ph.D. Candidate, Department of Aeronautical and Astronautical Engineering, Urbana, IL 61801 and Scientist, ERC Inc., Edwards AFB, CA 93524
** Professor, Department of Aeronautical and Astronautical Engineering, Urbana, IL 61801.
†Scientist, Space Vehicles Directorate, Kirtland AFB, NM 87117.
‡Scientist, Air Force Research Laboratory, Edwards AFB, CA 93524.

this study is an increased efficiency when the propellant operated at lower average temperatures.

Unfortunately, the thermocouple location behind the surface exposed to the plasma can only provide the steady state measurement of the bulk fuel temperature. The time resolution of these devices is also limited by the metal junction size. Additionally, any attempt to place thermocouples directly on the propellant surface exposes the thermocouple joint to the arc discharge. To obtain a time-resolved measurement of the surface temperature, we introduce a different approach. Photon detectors provide an unexplored alternative with the time-resolution required to investigate the micro-second discharges characteristic of these devices.

These detectors have found substantial use in the study of dynamic crack propagation, where they are used to evaluate conversion of work to heat at the tips of fast-moving cracks in solid materials.[6,7] Application of these detectors to the problem of an ablation-controlled arc requires significant analysis to determine the effects of the plasma and vapor layers, ablation characteristics of Teflon, proper selection of detector materials, and a validated means of translating the output voltages into temperatures.

As any black body heats, it emits radiation according to the Plank function.[8]

$$P_E = \frac{C_1}{\lambda^5\left(e^{\frac{C_2}{\lambda T}} - 1\right)} \qquad (1)$$

where C_1 is 3.742×10^8 W-μm^4/m^2, C_2 is 1.439×10^4 μm-K, λ is the radiation wavelength (μm), and T is the material temperature (K). Traces of the spectral emissive power for a black body at several relevant temperatures are shown in Figure 1.

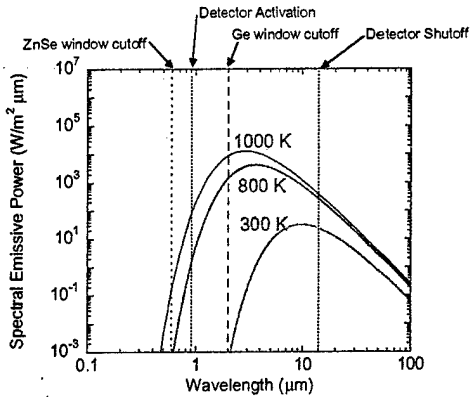

Figure 1: Several Plank distribution curves for blackbody emission at relevant temperatures.

Detector activation is shown at 900 nm along with the Ge transmission range (2-12 μm) and ZnSe transmission range (0.7-12 μm). Ge and ZnSe are window materials for infrared transmission. Multiplying the temperature curves by the wavelength dependent emissivity (ε_λ) provides an expected total emission from Teflon. Since Teflon emissivity is unknown, a rough estimate is used taking into account using only a stretching mode at 8.4 μm and its overtone at 4.4 μm. All values outside these effects are set at 0.01 such that there is some contribution though minimal. Detector responsivity is taken into account as a wavelength-varying term with the peak detector response (R_p) of 8.2 A/W at 10.5 μm.[9] The factory-supplied responsivity (D*) provides the wavelength dependence. These values must be integrated across the wavelength range of interest to determine an output current. However, the optical setup must be considered as well as the viewing geometry and preamplifier. The output voltage prediction is then calculated by

$$V = k_o GA(1 - \cos\theta)\int_\lambda \varepsilon_\lambda D^* R P_e d\lambda \qquad (2)$$

where k_o is an optics constant, G is the amplifier gain (20000 V/A), θ is the conical half angle defined by the diameter of and distance to the ZnSe window on the tank wall, A is the detector active area (80 μm x 80 μm), and P_e is given by Eqn. 1.

Temperature detection on an operating micro-PPT must account for a number of factors. Calibration of the output voltage

to the Teflon temperature must be accurate, and it must be verified experimentally that plasma exposure doesn't change the Teflon emissivity after firing. Also, emission from the plume must be separated from surface emission or a useful limit to the detector capabilities must be defined.

Actual measurement of the Teflon surface while the plasma is present may not be possible. Determination of plasma optical thickness for a Doppler broadened line[10] is given by (CGS units)

$$\tau = 1.76\times10^{-13}\lambda\left(\frac{Mc^2}{kT_e}\right)^{\frac{1}{2}} N_e l \qquad (3)$$

where M is the atomic mass (averaged to 16.7 AMU or $2.77\text{x}10^{-23}$ gm), c is the speed of light, k is the Boltzman constant, T_e is the electron temperature, N_e is the number density, and l is the plasma depth. τ is a non-dimensional number, for an optically thin plasma it is less than 1. Inserting typical values for a micro-PPT (N_e=$1\text{x}10^{16}$ cm^{-3}, T_e = 11500 K, l = 0.635 cm the thruster diameter, 6 μm wavelength), gives $\tau = 8\text{x}10^{4}$. This suggests that while the plasma is present any emission from the surface of the fuel will be absorbed before it can reach the detector.

Optical thickness of the plasma may not be the dominating problem. Broadband signal in the LWIR may be dominated by emission at some wavelengths that can mask the small Teflon signal and introduce a signal-to-noise problem while the plasma is present.

Experimental Apparatus

Detector

Experiments here are performed with a linear array of 4 80x80 μm HgCdTe detector elements.[9] The detectors are a p-n junction photodiode with pre-amplifier for each channel. Since the experiments detailed here are proof-of –concept material, sometimes only one or two channels are used to simplify the experimental setup. These detectors are housed in a liquid nitrogen dewar to minimize thermal noise from the substrate and support structure. A bias is applied to each detector at –5 mV.

Optics

The detector optics include a Newtonian telescope which images the surface of the fuel at 1:1 magnification over the detectors. The mirrors in the telescope are gold plated for 99% reflectivity in long-wave IR. A spherical mirror with a 304.8 mm focal length and a 50.8 mm diameter flat mirror are create the telescope. The detectors are kept at vacuum behind a ZnSe window with a 60° cone of view. A 25.4 mm diameter ZnSe window provides optical access into the vacuum chamber for thruster operation and calibration tests. During calibration, background thermal fluctuations are kept to a minimum by encasing the detector and telescope in a cardboard enclosure. The cardboard has aluminum foil attached to the outside to reflect infrared away from the setup.

Calibration

Detector calibration has gone through a number of iterations aimed at verifying that the calibration curve reflects only the emission from Teflon and not some other heat source. Early versions of the calibration had a Newtonian telescope looking down onto heated Teflon resting on copper on a hotplate. Since Teflon is quite transmissive in the wavelength range of interest, there was no way to verify that no signal from the heat source behind the Teflon was transmitting through and skewing the signal. Because of this, the current calibration version uses an 1/8" sheet of Teflon sandwiched between two copper plates with optical access holes .212" in diameter in both plates. Through the telescope the detectors are then imaged at 1:1 magnification onto the Teflon surface. The front plate is heated and there is no heat source behind the hole. Figure Figure 2 shows a schematic of this setup.

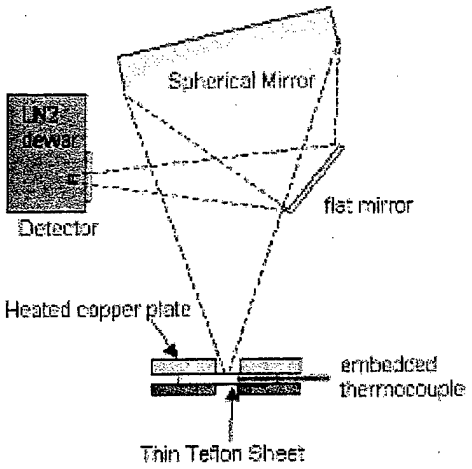

Figure 2: Pancake calibration provides Teflon heating with no rear heat source.

In practice, the calibration is performed at vacuum and an additional ZnSe tank window (25.4 mm DIA) limits the total observed emission. A typical calibration run takes about 10 hours since slow heating provides better uncertainty. Three type K thermocouples are drilled into the sides of the Teflon sheet and embedded close to the point where the detector is measuring. In early testing, the thermocouples touched the copper front plate, but it was shown that the copper and Teflon do not reach thermal equilibrium quickly.

An upper temperature limit to this technique so far has been experienced between 775-800 K. The reason for this limit is Teflon deformation as heating occurs. This deformation changes the viewing angle of the Teflon and therefore modifies the optical system. Theoretically, if the Teflon does not deform, the heating and cooling curves in the calibration should match, and in experimental cases without deformation, this has been shown to be the case. Use of springs to relieve pressure in the calibration jig is under consideration as a possible solution.

Thruster Measurement

For these tests a two electrode micro-PPT with 2.98 μF capacitor is used. Measurements of the surface are taken using the Newtonian telescope to image the surface onto the detectors. Targeting is performed via two wires crossed vertically and horizontally. The wires are tungsten with a 0.08 mm diameter. This cross is imaged for rough adjustment onto the detector. For fine adjustment, 1.2 A is run through each wire and the thermal signature is detected and maximized by adjusting the optics slightly.

Thruster configuration is a two electrode testbed with a 6.35 mm OD. A capacitive discharge typical of an LRC circuit generates the plasma at the exit plane of the thruster. To date, detection has only been performed on two electrode thrusters with fuel faces flush to the exit plane. Measurements on recessed thrusters would present additional difficulties with optical access.

For characterization of the plume, the viewing cone is focused over the surface of the micro-PPT without detecting the face. Figure 3 shows this geometry.

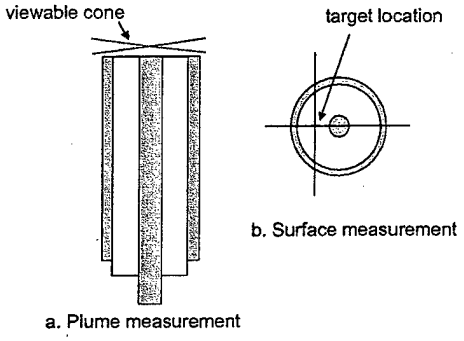

Figure 3: Optical view during plume tests (a.) is across the thruster exit plane. For surface tests (b.) crosshairs target the measurement.

For plume measurements, the center of the view cone must be targeted over the center electrode of the thruster. Due to arc spoking, the central electrode is the only location where plasma is always present.

Thruster surface data is targeted on Teflon between the two electrodes. Spatial resolution is simply the detector area since only 1:1 imaging is used. Figure 4a shows the detector images to scale on the micro-PPT face.

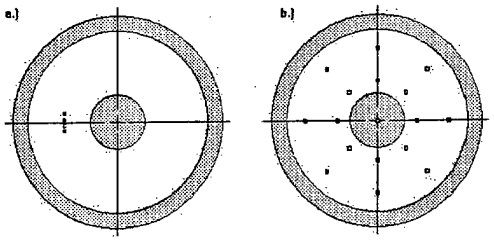

Figure 4: (a.) Linear and (b.) full coverage HgCdTe detector designs shown to scale on a micro-PPT face. The small squares are the detector images and the gray circles are the micro-PPT electrodes.

Due to spoking concerns, the small coverage area used by the 4-diode detector is not guaranteed to see the direct effects of the arc. Unless the IR measurements are correlated with photographs of the arc, it is difficult to determine what conditions the measured surface location is subjected to. To alleviate this problem, future measurements will be made using a detector with 16 elements in two concentric circles providing radial resolution at two locations and angular resolution every 45 degrees. Figure 4b shows this configuration.

Results and Discussion

Calibration

Practical application of the calibration process has defined a number of physical limitations. As the Teflon heats up it has a tendency to deform and possibly flow out of the calibration target hole. Figure 1a. and b. show two different cases of this problem. Figure 1c. shows a case where the Teflon did not deform through the test. The effect of this deformation is to change the viewing angle of the Teflon surface and invalidate the thermocouple readings at the detector imaging point.

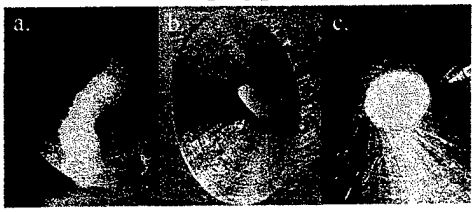

Figure 5: Teflon flows (a.) and extrudes (b.) though the calibration hole. In one case it remained flat (c.).

When this occurs, the detector voltage for the cooling portion significantly drops for a given temperature. In order to demonstrate that there is no significant chemical change that affects the emissivity as the Teflon heats and cools, a test without deformation must indicate heating and cooling curve matching. Figure 6 shows the full heating and cooling curves for two cases.

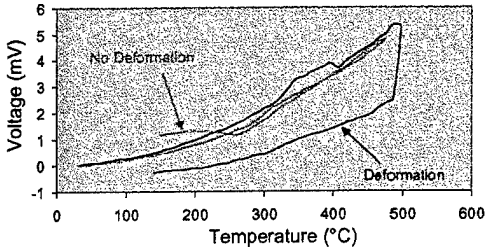

Figure 6: Calibration curves for cases where deformation occurs (blue) and does not (red).

The red plot is the case where Teflon deformation did not occur, and the heating and cooling curves match well. The cooling portion that fails to match at low temperatures is a symptom of the liquid nitrogen dewar warming up after <9 hours of testing. The blue plot shows a case where the Teflon deformed at 496 °C. The sharp drop-off indicates the extent to which the geometric view factor was compromised during this test. The heating curve, except for a variation from 320 to 400 °C, lines up fairly well with the non-deformation case.

The single case showing heating and cooling curve matching demonstrates that the heating curves can be valid for calibration purposes since Teflon deformation has been shown to be the source of discrepancy and is easily identifiable.

Figure 7 shows 3 heating curves for an experimental optical setup. For these curves, the optics are targeted once and the Teflon sample was placed in the exact same position for each test. High sensitivity to slight changes in optical setup has been noted. As such a constant optics setup from calibration to testing is crucial.

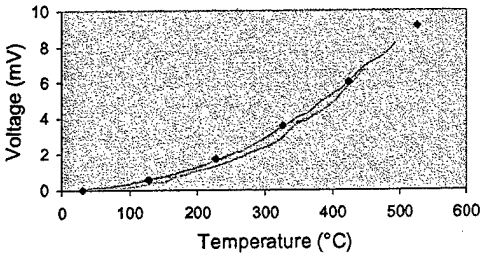

Figure 7: Calibration curves match well for the experimental optical setup.

Calibration Uncertainty

The heating curves shown above are analyzed for average and standard deviation. The standard deviation value is then root-mean-squared with the ±0.3 mV limitation of the detector to define a voltage uncertainty shown in Figure 8. Also shown are temperature uncertainties using the same method with the thermocouple uncertainty. For the K-type thermocouples used, uncertainty is ±2.2°C or .0075T, whichever is larger. The temperature uncertainty is difficult to see since it is about the same size as the data points used.

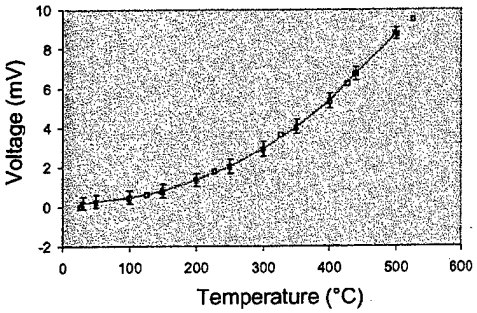

Figure 8: Calibration with typical uncertainty (red line) along with a calibration prediction (blue points).

Plasma Contribution

Note that data shown below does not correspond to the optical setup used to achieve the above calibration. Because of this, any direct comparison of the following data to the calibration curve above is meaningless.

For the plasma measurements, the focal point is located above the ablating fuel surface at varying distances from 1-7 mm. The results are shown in Figure 9.

At 3 mm from the fuel face the plume signal reaches a maximum. The 1 mm case also shows a plume signal, although it is consistently smaller than the 3 mm case. The signal from the plume drops into the noise at 5 mm from the fuel face indicating that the plume expansion at that point has limited the total emission that the detectors can sense. These measurements are all in terms of voltage since calibration with the plasma and neutral vapor has not been achieved.

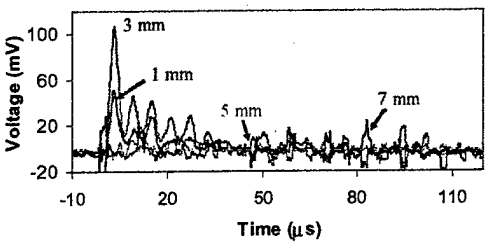

Figure 9: Typical observed plasma signals at varying distances from the fuel face.

Thruster Surface

Data shown for the thruster and plasma contribution is taken in a different optical setup from that used to define the calibration. Thruster data to match the calibration curve above is forthcoming. The plasma and surface contributions are measured according to the techniques shown in Figure 3.

Figure 10 shows a typical measurement of the fuel face plotted with the 3 mm plume data. Also plotted is the total energy to the arc from the capacitor.

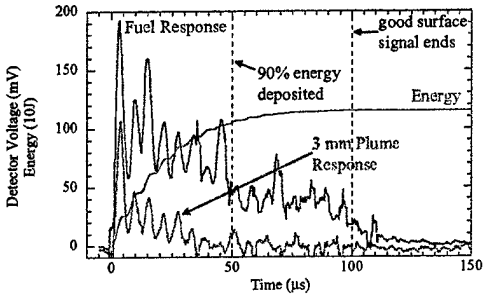

Figure 10: Plume and surface response with energy deposition over time.

Note that at ~50 µs (90% energy deposited) the signal from the plume ends. Most significantly, the signal from the fuel face is still appreciable out to ~100 µs.

This means that after the plume has stopped contributing to the signal, the signal remaining indicates that an actual surface temperature measurement is being made.

Conclusions

Experiment and analysis suggest that the physics underlying Teflon emission in the IR and detection with HgCdTe detectors are basically understood. The calibration procedure has been defined and validated, but the signal output thus far have been low due to restrictions on the optical setup used. Future calibrations will use optical systems redesigned to maximize the voltage output. The calibration procedure takes into account any effects not considered here such as the temperature dependence of emissivity for Teflon.

Initial measurements on a Teflon face exposed to an ablative discharge show promising results. Although these results are uncalibrated, the preliminary findings show a significant signal remaining after the end of the plume signal indicating a hot surface. During the early discharge, the noise involved with plasma emission may mask any signal from the surface preventing a measurement at peak energies. But mid- and post-discharge measurements are probably attainable. These measurements are significant for an evaluation of late-time ablation and to verify modeling assumptions about cooling characteristics.

Acknowledgements

This work is funded by the Air Force Research Laboratory at Edwards AFB, CA and performed at the Electric Propulsion Laboratory on-site. E. Antonsen acknowledges support from ERC Inc. Drs. M. Keidar and I. Boyd from the University of Michigan provided significant discussions concerning ablation physics. Both of these efforts are supported by AFOSR/NA. Dr. Mitat Birkan is the program manager. Additional thanks to the following people: Dr. W. Bro from DuPont Corporation provided material information on Teflon including infrared spectroscopy data. Dr. J. Lambros with the University of Illinois at Urbana-Champaign (UIUC) provided hands-on experience with HgCdTe detectors. Dr. D. Keefer of the University of Tennessee Space Institute (UTSI) provided information on plasma optical depths.

References

1. Spanjers, G.G., Bromaghim, D.R., Lake, Capt. J., Dulligan, M., White, D., Schilling, J.H., Bushman, S.S., Antonsen, E.L., Burton, R.L., Keidar, M., Boyd, I.D., "AFRL MicroPPT Development for Small Spacecraft Propulsion," AIAA Paper No. 2002-3974, Indianapolis, IN, July 2002.
2. Spanjers, G. G., Lotspeich, J. S., McFall, K. A., Spores, R. A., "Propellant losses Because of Particulate Emission in a Pulsed Plasma Thruster," *Journal of Propulsion and Power*, Vol. 14, No. 4, 1998, pp 554-559.
3. Burton, R. L., Rysanek, F., Antonsen, E. L., Wilson, M. J., Bushman, S. S., "Pulsed Plasma Thruster Performance for Microspacecraft Propulsion," Chap. 13, AIAA Progress Series, Micropropulsion for Small Spacecraft, M. Micci, ed., 2000.
4. Antonsen, E.L., Burton, R.L., Spanjers, G.G., Engelman, S.F., "Herriott Cell augmentation of a quadrature heterodyne interferometer," Rev. Sci. Instrum., 74 (1), Jan 2003.
5. Spanjers, G. G., Malak, J. B., Leiweke, R. J., Spores R. A., "The effect of propellant temperature on efficiency in a pulsed plasma thruster," Journal of Propulsion and Power, Vol. 14, No. 4, July-August 1998, 545-553.
6. Zehnder, A. T., Rosakis, A. J., "On the temperature distribution at the vicinity of dynamically propagating cracks in 4340 steel: experimental measurements using high-speed infrared detectors," *Journal of the Mechanics and Physics of Solids*, 39 (3), 385-417, 1991.
7. Mason, J. J., Rosakis, A. J., "On the dependence of the dynamic crack tip temperature fields in metals upon crack tip velocity and material parameters," *Mechanics of Materials*, 16 (4), 337-350, 1992.
8. Planck, M., *Theory of Heat Radiation*, Dover Publications, New York, 1959.
9. Fermionics, Simi Valley, CA, www.fermionics.com.

10. Book, D. L., Revised and Enlarged Collection of Plasma Physics Formulas and Data, NRL Memorandum Report 3332, 1977.